

Time-resolved molecular measurements reveal changes in astronauts during spaceflight.

Minzhang Zheng^{1,2}, Jacqueline Charvat³, Sara R. Zwart⁴, Satish Mehta⁵, Brian E. Crucian⁵, Scott M. Smith⁵, Jin He¹, Carlo Piermarocchi⁶ and George I. Mias^{1,2,6*}

¹*Department of Biochemistry and Molecular Biology, Michigan State University, East Lansing, Michigan, 48824, USA.

²Institute for Quantitative Health Science and Engineering, Michigan State University, East Lansing, Michigan, 48824, USA.
³KBR, Houston, Texas, 77058, USA.

⁴University of Texas Medical Center, Houston, Texas, 77555, USA.

⁵NASA Johnson Space Center, Houston, Texas, 77058, USA.

⁶*Department of Physics and Astronomy, Michigan State University, East Lansing, Michigan, 48824, USA.

*Corresponding author(s). E-mail(s): gmiias@msu.edu;

Abstract

From the early days of spaceflight to current missions, astronauts continue to be exposed to multiple hazards that affect human health, including low gravity, high radiation, isolation during long-duration missions, a closed environment and distance from Earth. Their effects can lead to adverse physiological changes and necessitate counter-measure development and/or longitudinal monitoring. A time-resolved analysis of biological signals can detect and better characterize potential adverse events during spaceflight, ideally preventing them and maintaining astronauts' wellness. Here we provide a time-resolved assessment of the impact of spaceflight on multiple astronauts (n=27) by studying multiple biochemical and immune measurements before, during, and after long-duration orbital spaceflight. We reveal space-associated changes of astronauts' physiology on both the individual level and across astronauts, including associations with bone resorption and kidney function, as well as immune-system dysregulation.

Keywords: astronaut, microgravity, time series, immune response, metabolites, nutrition

Introduction

As human space exploration continues to expand we anticipate an increasing number of long-duration and deep space missions. Beyond missions in low Earth orbit (LEO), plans are currently underway for a return to the moon, and utilizing such missions towards building a gateway for inter-planetary travel to Mars. Half a century of long-duration spaceflights on space stations has already demonstrated that such missions will pose several health risks to astronauts that have to be addressed. There are five categories of hazards faced by astronauts, that can directly contribute to health risks^{1,2}: (i) Transitioning from Earth's gravity to effective weightlessness or lower-than-Earth gravity. (ii) Experiencing higher levels of radiation, with considerably less shielding in the absence of Earth's protective magnetic field. (iii) Being in isolation during long-duration missions. (iv) Living in a closed environment with an evolving ecosystem for long periods of time. (v) Traveling and living at vast distances from Earth, where communications and facilities will be limited for direct health care assessment and intervention if necessary. The multiple physiological effects associated with these hazards include muscle and bone weakening, kidney stone risks and other problems due to fluid redistribution in the upper body, cancer risks due to radiation, immune dysregulation, cognitive and behavioral effects, and nutritional deficits²⁻⁴. All these hazards and associated risks dynamically change during space missions and necessitate close monitoring of crew members' health to ensure their safety and well-being.

Astronauts have experienced multiple clinical symptoms in long-duration LEO flights, with notable medical events reported in up to 46% of the crew members⁴. The most frequently reported events (defined as involving symptoms that are recurring or have prolonged duration, or are unresponsive to treatment), included cold sores, rashes, allergies, and infectious diseases⁴. Several studies aim to understand the molecular basis of these medical symptoms in long flights. Krieger et al.⁵ investigated cytokines in plasma and saliva in 13 astronauts during 4-6 month International Space Station (ISS) flights, and identified persistent immune dysregulation. Nutritional deficits have also been directly linked to space-related clinical symptoms and systemic physiological changes⁶. Smith et al. evaluated astronaut nutritional status during long stays on the ISS, identifying multiple marker changes associating bone resorption and oxidative damage across 11 astronauts⁷. Given the mission-critical role of maintaining astronaut health, the National Aeronautics and Space Administration (NASA) has developed the integrated medical model (IMM) as a tool for identifying medical conditions and quantifying medical risks to astronauts^{4,8,9}. Furthermore, the monitoring of standard medical physiological measurements, immune and metabolite markers, is now being supplemented with an expanding array of thousands of molecular measurements (omics) in individual astronauts. This was exemplified by the astronaut Twins Study¹⁰, which focused on molecular biology measurements to compare the effects of spaceflight on two twins, one on a 340-day mission, while the other was observed during this period on Earth. Multiple changes were

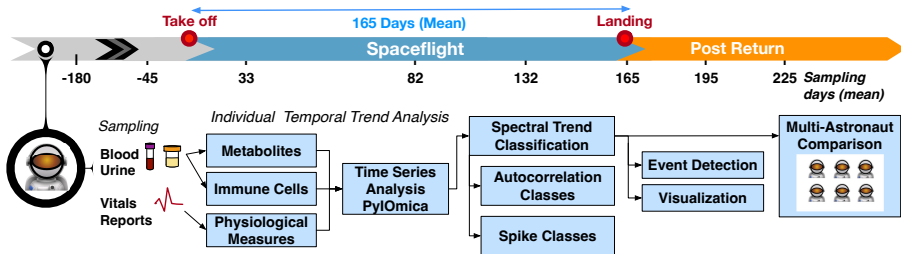


Fig. 1 Study overview. The study followed 27 astronauts across multiple long-duration missions (adjusted mean 165 days) on ISS. The data included multiple time measurements from 180 days pre-flight to two months post-flight for different blood and urine-detected molecules, as well immune cell characterizations, physiological measurements, and medical reports. The time-resolved measurements were analyzed per astronaut to identify temporal trends and detect events of interest. The individual measurements were finally used to construct a multi-astronaut comparison based on similar temporal changes across measurements.

observed giving a glimpse of how long-duration spaceflight affects an individual astronaut's physiology.

The next steps must enable monitoring of data from multiple astronauts during long-duration space missions, and should include the implementation of a personalized approach that can establish baseline characteristics in each crew member, detect deviations therefrom, and detect potentially adverse medical events. Such personalized monitoring of health based on omics have been implemented in the NASA Twins Study¹⁰, and on Earth, using blood¹¹, urine, saliva¹² and fecal samples. Testing methods have included microbiomes¹³, personalized coaching¹⁴ and digital devices¹⁵. In this investigation, we implemented the first (to our knowledge) multi-astronaut individual-focused monitoring in long-duration spaceflight. We characterized personal biological signals in 27 astronauts (8 female, 19 male) and assessed multiple metabolites, immune cell constitution, and physiological measurements spanning long-duration orbital missions (mean flight duration \sim 165 days), Figure 1. Using spectral-based methods^{12,16,17} we identified temporal trends, and classified multi-signal responses corresponding to in-flight and return to Earth changes. Our analysis addressed typical spaceflight research limitations, including monitoring issues that include uneven time sampling and missing data, as well as different sampling rates for different astronauts. We identified a set of time-resolved changes in metabolites and immune cell behavior that was concordant across the majority of astronauts, and associated with bone resorption, renal stone formation, T cell and monocyte dysregulation and nutritional deficiencies. Finally, we constructed a network assessing inter-astronaut similarities, identifying groups of astronauts with similar time-resolved trends and reported clinical symptoms. Our findings identify significant metabolite and immunological modifications during spaceflight, and suggest that individual-focused monitoring must be implemented to identify the onset of these changes in order to also address them in a timely manner with personalized countermeasures.

4 *Astronaut Molecular Monitoring*

Results

Astronaut cohort

We investigated time-resolved measurements from NASA astronauts across multiple missions to ISS. These astronauts had participated in two studies: the Nutritional Status Assessment and Validation of Procedures for Monitoring Crewmember Immune Function. These studies included multiple metabolic and physiological measurements (264 annotations), including blood and urine metabolite analyses and immune cellular assessments which were taken over multiple time-points before, during, and after flight.

This was a retrospective analysis of existing data. As part of our broader study on astronaut integrative data analysis, we identified 47 astronauts meeting the criteria of having multiple time-resolved measurements, and of those, 38 astronauts agreed to participate in our study following informed consent for this additional analysis. They had previously provided informed consent to participate in the original studies mentioned above. Out of these, 27 were found to have long-duration mission data (165 days mean) and were selected for analysis. Data were obtained for the Life Surveillance for Astronaut Health (LSAH) and Life Sciences Data Archive (LSDA).

Over the course of their missions, the astronauts experienced several clinical symptoms that were provided to our team as IMM reports. We aggregated the information across astronauts and events in Table 1. Events that resolved within the first 30 days of flight are classified as space adaptation symptoms⁴. The top space adaptation events included space motion sickness (14 astronauts), headache (10), and insomnia (9). The most frequent events later in the mission, categorized as non-adaptation events, included sleep disorder (15; reported 34 times), fatigue (14), and skin rash (9).

As is common, not only in spaceflight but with any medical monitoring outside laboratory settings, different measurements were available for different astronauts, with highly heterogeneous and uneven time sampling, and missing data. We created a common time sampling grid across all astronauts, where measurement data for each astronaut were summarized by time averages into nine adjusted mean-based timepoints: 180 and 45 days prior to flight, early flight (33 days), mid-flight (82 days) and late flight (132 days), return to Earth (after 165 days of flight), and 30 and 60 days following return. The common time grid was used to: (i) ensure non-attributability of data back to individual astronauts, since the time of flight is sometimes unique to each astronaut, and (ii) to enable the individual measurements to be comparable across astronauts.

Individual astronaut time-resolved assessment

We classified each astronaut's time-resolved measurement into different classes using spectral methods^{12,16,18} implemented in PyI0mica¹⁷. The approach allowed the identification of sets of measurements that display time-resolved deviations from an astronaut's baseline. This categorization provided 3 classes

of time trends: (i) *Lags*, for measurements showing statistically significant autocorrelation at different lags. Here an autocorrelation of a signal at a certain lag refers to a correlation of a signal with a delayed (lagged) version of itself. (ii-iii) *Spike Maxima or Minima* for measurements that do not belong in the *Lags* class, but have punctuated intensities (spikes) that are either high (Maxima) or low (Minima) at particular timepoints. The measurements assigned to these classes are further clustered into groups (G) and subgroups (S) based on their overall autocorrelation and signal intensity similarities respectively (see Methods).

The individual astronaut signal analyses are available in the Online Data Files (ODFs). Examples of the analysis are shown in Figure 2 for two astronauts. The heatmaps include the intensities of the measurements that had statistically significant (FDR < 0.05) trends for the Lag 1 class in two astronauts. Clustering of the data into groups (G) reveals similarities due to the signal autocorrelations, with the corresponding autocorrelation heatmap depicted on the right of the figure. The heatmap on the left depicts the intensities of the measurements and the final subgroup structure. For each subgroup, a summary of the time-resolved median structure is summarized with a graphical representation by a visibility graph¹⁹.

For astronaut 1, Figure 2a, there are changes associated with Lag 1 class. The main trend consists of upregulation of a subset of immune markers early in flight (Days 33 and 82), and a return to pre-flight levels after return to Earth. The changes are associated with with plasma concentrations of the cytokine CXCL5, CCL4, CXCL8, and TNF alpha, indicative of immune dysregulation (potential inflammation). Additionally, in urine there is an increase in sodium, chloride and zinc in early flight, returning to post-flight levels upon return to Earth. γ -carboxyglutamic acid (GLA) is decreased during flight, returning to pre-flight conditioning levels two months post return. GLA reflects post-translational modification of glutamic acid, and this modification is vitamin K dependent²⁰. On flights to the Russian space station Mir, vitamin K status in one crewmember was low during flight²¹ and subsequently vitamin K supplementation has been offered as a countermeasure for bone loss in astronauts. On ISS, this was not observed in a larger cohort of astronauts on longer missions²². In parallel, there is a decrease in immune cell levels, including CD8+ active and naïve relative percentages. This can be indicative of decreased immune response, as well as disruption of immune cell maturation cycles²³.

For astronaut 6 there are 3 sets of temporal patterns, Figure 2b, with changes associated with the Lag 1 class. In the first Group, MCH (mean corpuscular hemoglobin) and PYD (pyridinium cross-links) were found to increase during flight and stay high even following 2 months post return to earth. Increased MCH is associated with macrocytic anaemia. PYD is a bone resorption marker reflecting changes in bone metabolism and bone remodeling. With a symmetrically opposite trend, urine volume and testosterone decrease in flight and remain low for up to 2 months after return to Earth. The second set G2S1 indicates a gradual increase in intensities of H-peptide (another bone

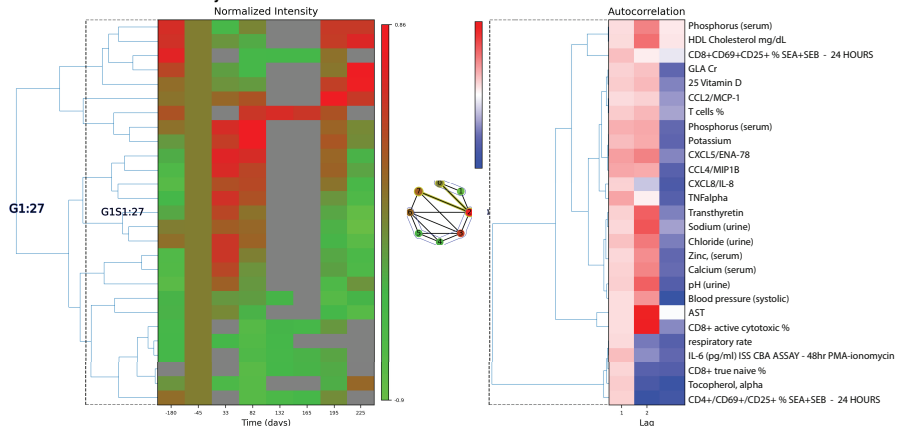
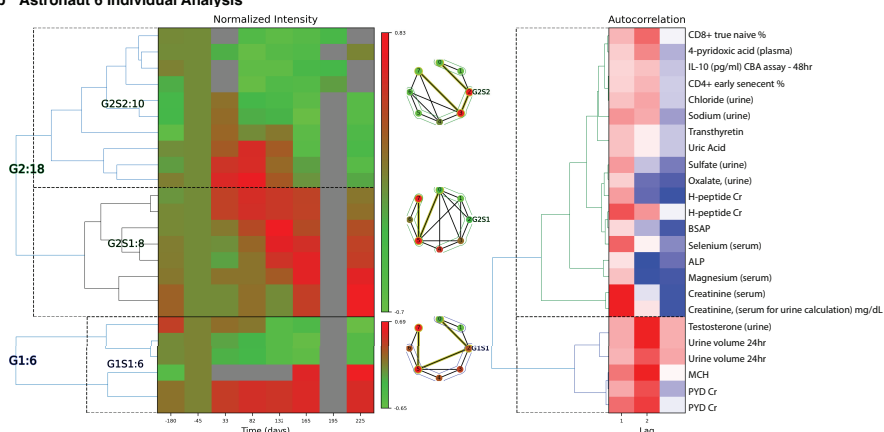
6 *Astronaut Molecular Monitoring***a Astronaut 1 Individual Analysis****b Astronaut 6 Individual Analysis**

Fig. 2 Individual Astronaut Examples. Classification results (Lag 1 patterns) are shown for astronaut 1 (a) and 6 (b). For each astronaut, we have: *Left heatmap*: Groups/sub-groups clustering of measurements, with adjusted mean time (with respect to takeoff). Times 165, 196 and 225 represent return to Earth, one and two months post-return respectively. *Middle graph*: Time-resolved visibility graph representation of median behavior within each group, with visibility-graph community detection identifying similar time behaviors¹⁹. *Right heatmap*: Autocorrelation clusters and annotations for the measurements identified. *ALP*: alkaline phosphatase, *BSAP*: bone-specific alkaline phosphatase, *CBA*: cytometric bead assay, *Cr*: creatinine normalized, *G*: group, *GLA*: gamma-carboxyglutamic acid, *MCH*: mean corpuscular hemoglobin, *PMA*: Phorbol 12-myristate 13-acetate, *PYD*: pyridinium cross-links, *S*: subgroup, *SEA*: staph enterotoxin A, *SEB*: staph enterotoxin B. *Multiple evaluations/repeats included*.

resorption marker), total and bone-specific alkaline phosphatase (BSAP), selenium, magnesium, and creatinine that persist after return to Earth. Probable indications include bone disease and kidney dysfunction, though certain values may be affected by dietary intake (e.g. magnesium). Finally, the third trend, G2S2 involves sets that show an increase in early flight but then consistent decreases in intensity that persist post flight. These include CD8+ T cell

'true naïve' and CD4+ T cell 'early senescent' relative percentages, that may indicate immune cell maturation dysregulation. IL-10 also remains reduced post flight, as compared to preflight baseline concentrations. Other compounds with similar trends include 4-pyridoxic acid, chloride and sodium in urine, transthyretin, uric acid, and sulfate and oxalate levels (in urine).

The results for all astronauts showed similar patterns, indicative of individual-specific changes particularly associated with early spaceflight or landing stress, with multiple changes persisting up to two months following return to Earth. Further details and representations of the trends identified for each astronaut are available in deidentified plots and tables in the ODFs.

Spaceflight effects across multiple astronauts

To identify similarities across astronauts, we investigated how often the individual-astronaut statistically significant signals were identified across multiple astronauts. The top measurements by incidence (≥ 16), are shown in Table 2, including a trend summary and potential physiological aspects.

Multiple signals showed similar trends across individuals. The top examples are shown in Figure 3a-i across all measurements, as well as for immune cells, Figure 3j-l. The results from PYD are prominent and most prevalent (observed in 21 astronauts), Figure 3a, showing an increase in intensity beginning early in spaceflight, and also persisting post flight (at least for 30 days). PYD is a marker of bone resorption and is indicative of the ongoing concern of bone loss among astronauts on long-duration spaceflights^{7,24-27}. We also observe fluctuations and a decrease in urinary sodium, Figure 3a, that indicates retention - particularly upon return to Earth, and this may be related to the effects of microgravity on body fluid balance, as also seen in urine volume Figure 3d.

Zinc in serum, Figure 3c, is elevated during flight, and returns to low levels after return to Earth²⁸. While zinc serum is not an indicator of nutritional zinc levels²⁹, the fluctuations may have health implications, as long term elevated zinc can induce nausea and headaches and gastrointestinal problems, potentially leading to decreased immune function and copper deficiency, while zinc deficiency could be an issue after return to Earth³⁰.

Potassium levels were found to be generally lower (but elevated for a small subset of astronauts during flight), with a sharp decrease across astronauts upon return to earth. This was also reported for short Apollo missions³¹, and the connections between muscle loss, kidney dysfunction and cardiovascular conditions need to be investigated further³².

Iron in serum, Figure 3f, appears affected by landing events as there is a marked decrease post return to Earth indicative of potential disruption of iron metabolism, which could lead to anemia and affect the immune response³³. There is also an increase in relative iron levels during flight for some astronauts, that may be related to neocytolysis³⁴. Diastolic blood pressure, Figure 3g, is reduced during space flight across astronauts; this transient in-flight effect has also been reported in a smaller cohort ($n=12$)³⁵ and could have implications for hypotension during flight (though returning to normal levels following

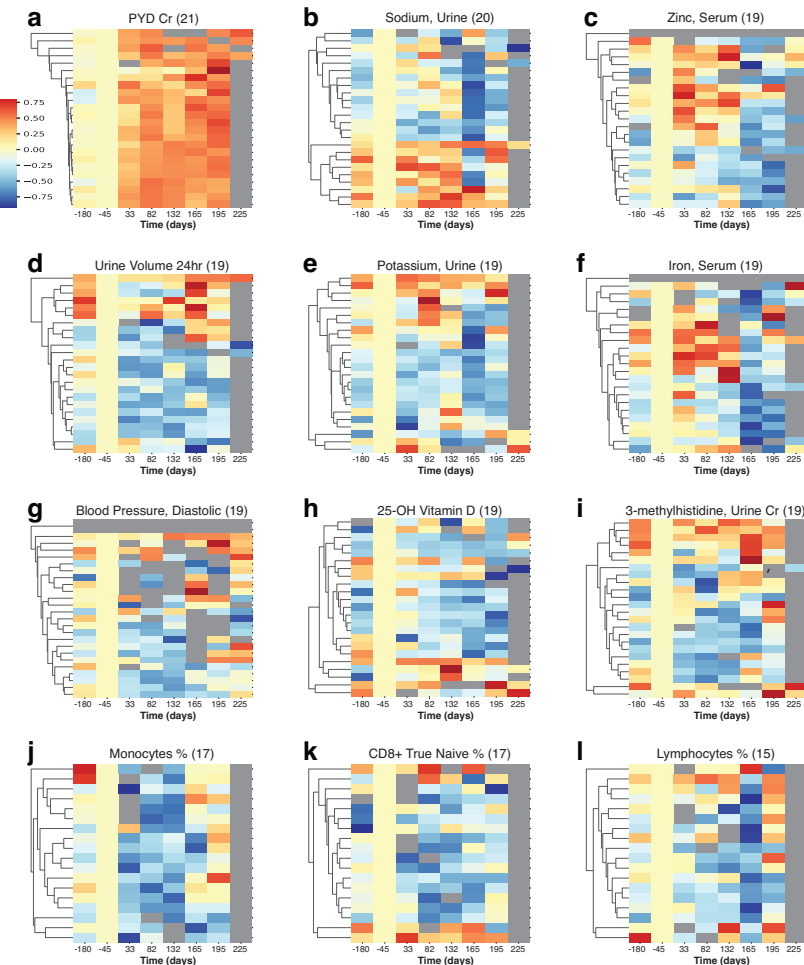


Fig. 3 Multiple measurements show similar trends across astronauts. The heatmaps represent the normalized intensities of each measurement across all astronauts (rows) over time (columns). These measurements were identified to show statistically significant trends (FDR < 0.05) in multiple crew members, with the respective astronaut tallies shown in parentheses. a-i are the top measurements by frequency overall, and j-l are the top immune cell measurements. PYD: pyridinium cross links, Cr: normalized with creatinine.

Earth return). 25-OH Vitamin D measurements are decreased across 19 astronauts, consistent with concerns relating to bone health⁷. 3-methylhistidine (3-MH), normalized with creatinine³⁶, was generally decreased during spaceflight, showing some increase in levels on landing for a subset of astronauts. An increase of 3-MH would be consistent with skeletal muscle degradation³⁷, and the overall 3-MH changes in flight, particularly punctuated on landing require further investigation.

In terms of immune cells, we noticed a general decrease in Figure 3j-l, in monocyte, CD8+ naïve T cell, and ‘bulk’ lymphocyte relative percentages.

This decrease highlights the potential for immune related disorders^{23,38,39}. This finding could also be linked the (largely) asymptomatic reactivation of latent herpesviruses, as has previously been observed in ISS astronauts during spaceflight³⁹. It should be noted, that recently atopic dermatitis in some astronaut cases has been positively correlated with latent herpesvirus reactivation, in particular HSV1⁴⁰. Recently, Mourad et al., 2022, postulated that reactivation of VZV occurred in mothers, who experienced an asymptomatic reactivation of herpes zoster virus, similar to that described in astronauts⁴¹⁻⁴³.

Additionally, we investigated whether the common temporal trends across astronauts could provide a grouping of astronauts based on similar physiological responses, by studying the structure of a multi-astronaut network¹⁸. In the constructed network, Figure 4, nodes depict astronauts (n=24) for which time series data were matched, while weighted edges represent how many measurements showed similarity (Euclidean distance) in their signal periodograms across pairs of astronauts. The five shown communities (labeled Community 0 through Community 4) were detected using a k-means approach, with k=5 (see Methods). While the number of astronauts included (n=24) restricts findings, we still observed community separations (except Community 4, which is a singleton), with distinct characteristics. The largest group, Community 0 included 7 male and 1 female astronaut. Weighted edges indicate that H Peptide drove the similarity within Community 0. During flight, the astronauts of Community 0 had reported space motion sickness predominantly (5 times) as well as sleep disorder, insomnia and headaches (4 times each). The second largest group (Community 1), is evenly balanced based on sex (3 male, 3 female). The clustering is dominated by MCV (mean corpuscular volume) behavior, and the members predominantly reported sleep disorder (5 times), as well as space motion sickness and skin rash (3 times each). Similarly, in Community 2 (3 male, 1 female) the astronauts reported insomnia and headaches (3 times each), while for Community 3 (3M, 2F) sleep disorder (4 times), and nasal congestion, shoulder sprain/strain and headache (3 times).

Discussion

We have implemented an individual-focused approach to investigate personalized astronaut monitoring and detecting deviations from a wellness baseline. The astronauts experienced physiological changes that are associated with the identified molecular markers. The time-resolved analysis revealed the majority of changes to be associated with space stay, and also with the impact and stress of landing prior to readjustment to return to Earth. The impacted measurements are related to microgravity adaptation adverse effects such as bone resorption and kidney function, and to immune-system dysregulation. These changes suggest further countermeasures are necessary to prevent adverse outcomes (e.g. osteoporosis, renal stones, viral reactivation), particularly on long-duration flights. These can include enhanced food provisions, or if required, nutritional supplementation, as well as provision of relevant immune-disorder medications on board.

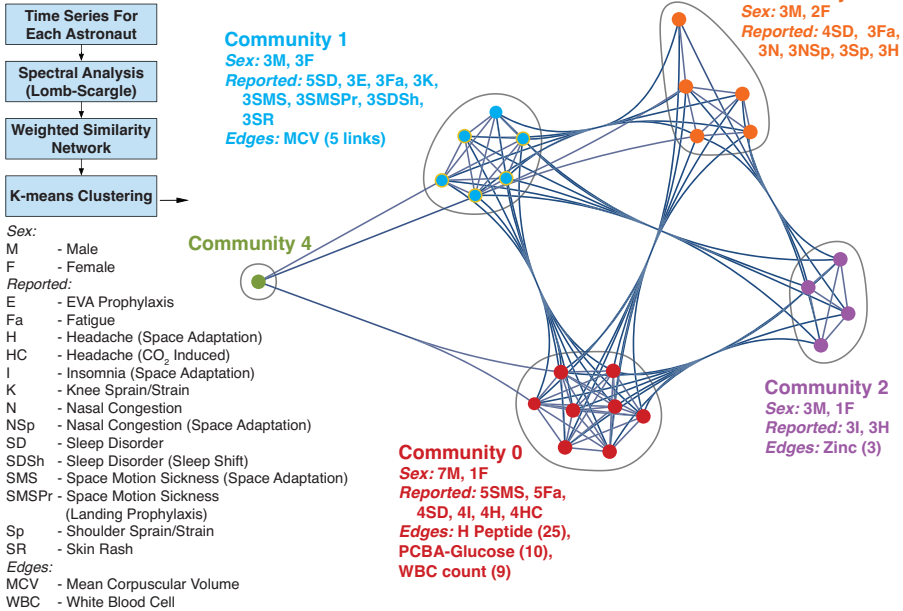
Across-Astronaut Community Detection

Fig. 4 Astronaut Temporal Communities. Using the time-resolved measurements a network was constructed to identify communities of astronauts with similar temporal behavior. The nodes in the network represent astronauts, while the weighted edges correspond to different measurements, weighted with the number of astronaut pairs for which the time behavior is similar. Four Communities were identified (0-3) and a singleton, denoted in different colors. The male/female count, top reported IMM clinical symptoms, and edges (with corresponding counts/weights) associated with each community are included.

Our successful detection of individual-astronaut changes offers an extensible approach that can be used to integrate multiple time-resolved measurements (omics, physiological measurements, mobile device temporal data, and any temporal signal) on individual astronauts towards detecting and preventing potentially harmful medical events. By cataloguing such event onsets and associated measurement responses, the non-wellness transitions in astronauts can be used for providing timely diagnosis and countermeasures during space missions. This is vital during long-duration deep space missions, where distance from Earth necessitates self-reliance by astronaut crews to maintain their own wellness, as we expand space exploration to Mars and beyond.

Tables

Table 1 Integrated Medical Model Reports

| Reported Condition | Astronauts | Total Events |
|---|------------|--------------|
| Sleep Disorder | 15 | 34 |
| Space Motion Sickness (Space Adaptation) | 14 | 14 |
| Fatigue | 14 | 23 |
| Headache (Space Adaptation) | 10 | 10 |
| Skin Rash | 9 | 11 |
| Insomnia (Space Adaptation) | 9 | 9 |
| Skin Abrasion | 8 | 12 |
| Nasal Congestion | 8 | 10 |
| Back Sprain/Strain | 8 | 15 |
| Sleep Disorder due to Sleep Shift | 7 | 7 |
| Nasal Congestion (Space Adaptation) | 7 | 7 |
| Knee Sprain/Strain | 7 | 16 |
| Headache (CO ₂ Induced) | 7 | 9 |
| Allergic Reaction (Mild to Moderate) | 7 | 11 |
| Shoulder Sprain/Strain | 6 | 7 |
| Paresthesias | 6 | 7 |
| Space Motion Sickness Landing Prophylaxis | 5 | 5 |
| Eye Irritation/Abrasion | 5 | 8 |
| Elbow Sprain/Strain | 5 | 10 |
| Constipation (Space Adaptation) | 5 | 5 |
| Constipation | 5 | 7 |
| Back Pain (Space Adaptation) | 5 | 5 |

12 *Astronaut Molecular Monitoring***Table 2** Aggregated Measurements Across Astronauts.

| Measurement (fluid) ^a | Count ^b | F,R,PR Trends ^{c,d} | Physiological Aspects |
|----------------------------------|--------------------|------------------------------|--|
| Pyridinium (PYD) Cr | 21 | ↑ ↑ ↑ | Bone resorption ²⁴⁻²⁶ |
| Sodium (urine) | 20 | — — ↓ (↑ ↓ —) | Saline ingestion pre-landing |
| Zinc (serum) | 19 | ↑ ↓ ↓ (↓ ↓ ↓) | Nausea; bone resorption ²⁸ ; immune response, wound healing ³⁰ |
| Urine volume 24 hour | 19 | ↓ ↓ ↓ (↓ ↑ —) | Inadequate fluid intake; fluid redistribution; renal stones ²⁶ |
| Potassium (urine) | 19 | ↓ ↓ ↓ (↑ ↓ ↓) | Retention - renal stones; muscle disuse ³² |
| Iron (serum) | 19 | ↑ ↓ ↓ (— ↓ ↓) | Iron metabolism; immune response ^{33,34} |
| Blood pressure diastolic | 19 | ↓ ↑ — | Hypotension; conditioning ³⁵ |
| 25-OH Vitamin D | 19 | ↓ ↓ ↓ | Bone mass resorption ⁷ |
| 3-methylhistidine (urine) Cr | 19 | ↓ ↓ ↑ (— ↑ —) | Skeletal muscle maintainance ³⁷ |
| Sodium | 18 | ↓ — — (↑ — ↑) | Fluid imbalance; diet |
| Creatinine (serum) | 18 | ↓ ↓ ↓ (↑ — —) | Muscle mass; diet ^{44,45} |
| Chloride (urine) | 18 | — ↓ ↓ (↑ ↓ —) | Dietary salt; saline ingestion (end of mission); intravenous saline at landing |
| Blood pressure systolic | 18 | ↓ ↑ — | Hypotension; conditioning ³⁵ |
| Vitamin B12 | 17 | ↓ ↓ ↓ (↑ ↑ —) | Food absorption, neurological manifestation, ocular health ^{6,46,47} |
| Transferrin receptors | 17 | ↓ ↓ ↑ | Iron metabolism shifts ⁷ |
| Sulfate (urine) | 17 | ↓ ↓ ↓ (↑ ↑ ↑) | Urinary supersaturation; diet |
| pH (urine) | 17 | ↓ ↓ ↓ (↑ ↑ —) | Kidney issues; renal stones ²⁶ |
| Monocytes % | 17 | ↓ ↓ — | Immunity; viral reactivation |
| Magnesium (serum) | 17 | ↑ ↓ — (↓ ↓ —) | Decreased intake; renal stones ⁷ |
| CD8+ true naïve % | 17 | ↓ ↓ ↓ | T cell maturation dysregulation ²³ |
| Phosphorus (urine) | 16 | ↓ ↓ ↓ (↑ ↓ —) | Renal; skeletal ^{6,7,48} |
| γ-carboxyglutamic acid Cr | 16 | — ↑ ↑ (↓ ↓ ↑) | Vitamin K status ²⁰⁻²² |
| Calcium (serum) | 16 | ↓ ↓ ↓ (↓ ↑ —) | Bone metabolism; renal stone risk ²⁶ |

^aCr: normalized using creatinine.^bCount of individuals for which measurement has a statistically significant trend.^cThe majority signal intensity trend is summarized with respect to preflight for: Flight (F), Return date (R), Post-return (PR) sequentially. If a secondary trend is observed it is listed in the parenthesis.^dThe intensity trends are: same as preflight (—), higher intensity (↑), or lower intensity(↓).

Acknowledgements

This project was supported by the Translational Research Institute for Space Health (TRISH) through NASA Cooperative Agreement NNX16AO69A (project T0412, PI: GI Mias). CP acknowledges support by NIH R01GM122085. The Nutritional Status Assessment SMO (PI: SM Smith) and the Validation of Procedures for Monitoring Crewmember Immune Function (PI: BE Crucian) were supported by the NASA Human Research Program Human Health Countermeasures Element.

Author Contributions

Conceptualization, MZ, CP and GIM; Methodology, MZ, CP and GIM; Software, MZ and GIM; Investigation, MZ, JC, JH, SRZ, SM, BEC, SMS, CP and GIM; Visualization, MZ, GIM; Resources, MZ and GIM; Writing – Original Draft, GIM; Writing – Review & Editing, MZ, JC, JH, SRZ, SM, BEC, SMS, CP and GIM; Funding Acquisition, CP and GIM; Supervision, GIM.

Competing Interests

JC is employed by KBR. MZ, JH, SRZ, SM, BEC, SMS, JH, CP and GIM declare the absence of any commercial or financial relationships that could be construed as a potential conflict of interest.

References

- [1] Afshinnekoo, E., Scott, R.T., MacKay, M.J., Pariset, E., Cekanaviciute, E., Barker, R., Gilroy, S., Hassane, D., Smith, S.M., Zwart, S.R., Nelman-Gonzalez, M., Crucian, B.E., Ponomarev, S.A., Orlov, O.I., Shiba, D., Muratani, M., Yamamoto, M., Richards, S.E., Vaishampayan, P.A., Meydan, C., Foox, J., Myrrhe, J., Istasse, E., Singh, N., Venkateswaran, K., Keune, J.A., Ray, H.E., Basner, M., Miller, J., Vitaterna, M.H., Taylor, D.M., Wallace, D., Rubins, K., Bailey, S.M., Grabham, P., Costes, S.V., Mason, C.E., Beheshti, A.: Fundamental biological features of space-flight: Advancing the field to enable deep-space exploration. *Cell* **183**(5), 1162–1184 (2020). <https://doi.org/10.1016/j.cell.2020.10.050>
- [2] Patel, Z.S., Brunstetter, T.J., Tarver, W.J., Whitmire, A.M., Zwart, S.R., Smith, S.M., Huff, J.L.: Red risks for a journey to the red planet: The highest priority human health risks for a mission to mars. *NPJ Microgravity* **6**(1), 33 (2020). <https://doi.org/10.1038/s41526-020-00124-6>
- [3] Baker, E.S., Barratt, M.R., Sams, C.F., M.L., W.: Human response to space flight. In: Barratt, M.R., Baker, E.S., Pool, S.L. (eds.) *Principles of Clinical Medicine for Space Flight*, pp. 367–411. Springer, New York (2019)
- [4] Crucian, B., Babiak-Vazquez, A., Johnston, S., Pierson, D.L., Ott, C.M., Sams, C.: Incidence of clinical symptoms during long-duration orbital spaceflight. *Int J Gen Med* **9**, 383–391 (2016). <https://doi.org/10.2147/IJGM.S114188>
- [5] Krieger, S.S., Zwart, S.R., Mehta, S., Wu, H., Simpson, R.J., Smith, S.M., Crucian, B.: Alterations in saliva and plasma cytokine concentrations during long-duration spaceflight. *Front Immunol* **12**, 725748 (2021). <https://doi.org/10.3389/fimmu.2021.725748>
- [6] Smith, S.M., Zwart, S.R., Douglas, G.L., Heer, M.: *Human Adaptation to Space Flight: The Role of Food and Nutrition*, 2nd edn. National Aeronautics and Space Administration, Lyndon B. Johnson Space Center. (2021)
- [7] Smith, S.M., Zwart, S.R., Block, G., Rice, B.L., Davis-Street, J.E.: The nutritional status of astronauts is altered after long-term space flight aboard the international space station. *J Nutr* **135**(3), 437–43 (2005). <https://doi.org/10.1093/jn/135.3.437>
- [8] Keenan, A., Young, M., Saile, L., Boley, L., Walton, M., Kerstman, E., Shah, R., Goodenow, D.A., Myers Jr, J.G.: The integrated medical model: A probabilistic simulation model predicting in-flight medical risks. (2015). 45th International Conference on Environmental Systems

[9] Antonsen, E.L., Myers, J.G., Boley, L., Arellano, J., Kerstman, E., Kadwa, B., Buckland, D.M., Van Baalen, M.: Estimating medical risk in human spaceflight. *npj Microgravity* **8**(1), 8 (2022). <https://doi.org/10.1038/s41526-022-00193-9>

[10] Garrett-Bakelman, F.E., Darshi, M., Green, S.J., Gur, R.C., Lin, L., Macias, B.R., McKenna, M.J., Meydan, C., Mishra, T., Nasrini, J., Piening, B.D., Rizzardi, L.F., Sharma, K., Siamwala, J.H., Taylor, L., Vitaterna, M.H., Afkarian, M., Afshinnekoo, E., Ahadi, S., Ambati, A., Arya, M., Bezdan, D., Callahan, C.M., Chen, S., Choi, A.M.K., Chlipala, G.E., Contrepois, K., Covington, M., Crucian, B.E., De Vivo, I., Dinges, D.F., Ebert, D.J., Feinberg, J.I., Gandara, J.A., George, K.A., Goutsias, J., Grills, G.S., Hargens, A.R., Heer, M., Hillary, R.P., Hoofnagle, A.N., Hook, V.Y.H., Jenkinson, G., Jiang, P., Keshavarzian, A., Laurie, S.S., Lee-McMullen, B., Lumpkins, S.B., MacKay, M., Maienschein-Cline, M.G., Melnick, A.M., Moore, T.M., Nakahira, K., Patel, H.H., Pietrzyk, R., Rao, V., Saito, R., Salins, D.N., Schilling, J.M., Sears, D.D., Sheridan, C.K., Stenger, M.B., Tryggvadottir, R., Urban, A.E., Vaisar, T., Van Espen, B., Zhang, J., Ziegler, M.G., Zwart, S.R., Charles, J.B., Kundrot, C.E., Scott, G.B.I., Bailey, S.M., Basner, M., Feinberg, A.P., Lee, S.M.C., Mason, C.E., Mignot, E., Rana, B.K., Smith, S.M., Snyder, M.P., Turek, F.W.: The nasa twins study: A multidimensional analysis of a year-long human spaceflight. *Science* **364**(6436) (2019). <https://doi.org/10.1126/science.aau8650>

[11] Chen, R., Mias, G.I., Li-Pook-Than, J., Jiang, L., Lam, H.Y., Chen, R., Miriami, E., Karczewski, K.J., Hariharan, M., Dewey, F.E., Cheng, Y., Clark, M.J., Im, H., Habegger, L., Balasubramanian, S., O'Huallachain, M., Dudley, J.T., Hillenmeyer, S., Haraksingh, R., Sharon, D., Euskirchen, G., Lacroix, P., Bettinger, K., Boyle, A.P., Kasowski, M., Grubert, F., Seki, S., Garcia, M., Whirl-Carrillo, M., Gallardo, M., Blasco, M.A., Greenberg, P.L., Snyder, P., Klein, T.E., Altman, R.B., Butte, A.J., Ashley, E.A., Gerstein, M., Nadeau, K.C., Tang, H., Snyder, M.: Personal omics profiling reveals dynamic molecular and medical phenotypes. *Cell* **148**(6), 1293–1307 (2012). <https://doi.org/10.1016/j.cell.2012.02.009>

[12] Mias, G.I., Singh, V.V., Rogers, L.R.K., Xue, S., Zheng, M., Doman-skyi, S., Kanada, M., Piermarocchi, C., He, J.: Longitudinal saliva omics responses to immune perturbation: a case study. *Sci Rep* **11**(1), 710 (2021). <https://doi.org/10.1038/s41598-020-80605-6>

[13] Zhou, W., Sailani, M.R., Contrepois, K., Zhou, Y., Ahadi, S., Leopold, S.R., Zhang, M.J., Rao, V., Avina, M., Mishra, T., Johnson, J., Lee-McMullen, B., Chen, S., Metwally, A.A., Tran, T.D.B., Nguyen, H., Zhou, X., Albright, B., Hong, B.Y., Petersen, L., Bautista, E., Hanson, B., Chen, L., Spakowicz, D., Bahmani, A., Salins, D., Leopold, B., Ashland,

16 *Astronaut Molecular Monitoring*

M., Dagan-Rosenfeld, O., Rego, S., Limcaoco, P., Colbert, E., Allister, C., Perelman, D., Craig, C., Wei, E., Chaib, H., Hornburg, D., Dunn, J., Liang, L., Rose, S.M.S., Kukurba, K., Piening, B., Rost, H., Tse, D., McLaughlin, T., Sodergren, E., Weinstock, G.M., Snyder, M.: Longitudinal multi-omics of host-microbe dynamics in prediabetes. *Nature* **569**(7758), 663–671 (2019). <https://doi.org/10.1038/s41586-019-1236-x>

[14] Price, N.D., Magis, A.T., Earls, J.C., Glusman, G., Levy, R., Lausted, C., McDonald, D.T., Kusebauch, U., Moss, C.L., Zhou, Y., Qin, S., Moritz, R.L., Brogaard, K., Omenn, G.S., Lovejoy, J.C., Hood, L.: A wellness study of 108 individuals using personal, dense, dynamic data clouds. *Nat Biotechnol* **35**(8), 747–756 (2017). <https://doi.org/10.1038/nbt.3870>

[15] Li, X., Dunn, J., Salins, D., Zhou, G., Zhou, W., Schussler-Fiorenza Rose, S.M., Perelman, D., Colbert, E., Runge, R., Rego, S., Sonecha, R., Datta, S., McLaughlin, T., Snyder, M.P.: Digital health: Tracking physiomes and activity using wearable biosensors reveals useful health-related information. *PLoS Biol* **15**(1), 2001402 (2017). <https://doi.org/10.1371/journal.pbio.2001402>

[16] Mias, G.I., Yusufaly, T., Roushangar, R., Brooks, L.R., Singh, V.V., Christou, C.: MathIOmica: An Integrative Platform for Dynamic Omics. *Sci Rep* **6**, 37237 (2016). <https://doi.org/10.1038/srep37237>

[17] Domanskyi, S., Piermarocchi, C., Mias, G.I.: PyIOmica: longitudinal omics analysis and trend identification. *Bioinformatics* **36**(7), 2306–2307 (2019) <https://academic.oup.com/bioinformatics/article-pdf/36/7/2306/33027234/btz896.pdf>. <https://doi.org/10.1093/bioinformatics/btz896>

[18] Zheng, M., Piermarocchi, C., Mias, G.I.: Temporal response characterization across individual multiomics profiles of prediabetic and diabetic subjects. *Sci Rep* **12**(1), 12098 (2022). <https://doi.org/10.1038/s41598-022-16326-9>

[19] Zheng, M., Domanskyi, S., Piermarocchi, C., Mias, G.I.: Visibility graph based temporal community detection with applications in biological time series. *Scientific Reports* **11**(1), 1–12 (2021). <https://doi.org/10.1038/s41598-021-84838-x>

[20] Furie, B., Bouchard, B.A., Furie, B.C.: Vitamin k-dependent biosynthesis of gamma-carboxyglutamic acid. *Blood* **93**(6), 1798–808 (1999)

[21] Caillot-Augusseau, A., Vico, L., Heer, M., Voroviev, D., Souberbielle, J.C., Zitterman, A., Alexandre, C., Lafage-Proust, M.H.: Space flight is associated with rapid decreases of undercarboxylated osteocalcin and increases of markers of bone resorption without changes in their circadian variation:

observations in two cosmonauts. *Clin Chem* **46**(8 Pt 1), 1136–43 (2000)

[22] Zwart, S.R., Booth, S.L., Peterson, J.W., Wang, Z., Smith, S.M.: Vitamin k status in spaceflight and ground-based models of spaceflight. *J Bone Miner Res* **26**(5), 948–54 (2011). <https://doi.org/10.1002/jbmr.289>

[23] Crucian, B., Stowe, R.P., Mehta, S., Quirriarte, H., Pierson, D., Sams, C.: Alterations in adaptive immunity persist during long-duration spaceflight. *NPJ Microgravity* **1**, 15013 (2015). <https://doi.org/10.1038/npjmgrav.2015.13>

[24] Caillot-Augusseau, A., Lafage-Proust, M.H., Soler, C., Pernod, J., Dubois, F., Alexandre, C.: Bone formation and resorption biological markers in cosmonauts during and after a 180-day space flight (euromir 95). *Clin Chem* **44**(3), 578–85 (1998)

[25] Smith, S.M., Nillen, J.L., Leblanc, A., Lipton, A., Demers, L.M., Lane, H.W., Leach, C.S.: Collagen cross-link excretion during space flight and bed rest. *J Clin Endocrinol Metab* **83**(10), 3584–91 (1998). <https://doi.org/10.1210/jcem.83.10.5169>

[26] Smith, S.M., Heer, M., Shackelford, L.C., Sibonga, J.D., Spatz, J., Pietrzyk, R.A., Hudson, E.K., Zwart, S.R.: Bone metabolism and renal stone risk during international space station missions. *Bone* **81**, 712–720 (2015). <https://doi.org/10.1016/j.bone.2015.10.002>

[27] Man, J., Graham, T., Squires-Donelly, G., Laslett, A.L.: The effects of microgravity on bone structure and function. *NPJ Microgravity* **8**(1), 9 (2022). <https://doi.org/10.1038/s41526-022-00194-8>

[28] Cann, C.E., Adachi, R.R.: Bone resorption and mineral excretion in rats during spaceflight. *Am J Physiol* **244**(3), 327–31 (1983). <https://doi.org/10.1152/ajpregu.1983.244.3.R327>

[29] Hennigar, S.R., Lieberman, H.R., Fulgoni, r. V. L., McClung, J.P.: Serum zinc concentrations in the us population are related to sex, age, and time of blood draw but not dietary or supplemental zinc. *J Nutr* **148**(8), 1341–1351 (2018). <https://doi.org/10.1093/jn/nxy105>

[30] National Institutes of Health, Office of Dietary Supplements: Zinc - Health Professional Fact Sheet (2022). <https://ods.od.nih.gov/factsheets/Zinc-HealthProfessional/> Accessed 2022-04-09

[31] W.C., A., C.S., L., C.L., F.: Clinical biochemistry. In: S., J.R., F., D.L., A., B.C. (eds.) *Biomedical Results of Apollo* (NASA SP-368), pp. 185–196. Scientific and Technical Information Office, National Aeronautics and Space Administration, Washington, D.C. (1975)

18 *Astronaut Molecular Monitoring*

- [32] Lane, H.W., C., L., M., S.S.: Fluid and electrolyte homeostasis. In: Lane, H.W., Schoeller, D.A. (eds.) *Nutrition in Spaceflight and Weightlessness Models*, pp. 119–39. CRC Press, Boca Raton (2000)
- [33] Dallman, P.R.: Iron deficiency and the immune response. *Am J Clin Nutr* **46**(2), 329–34 (1987). <https://doi.org/10.1093/ajcn/46.2.329>
- [34] Alfrey, C.P., Rice, L., Udden, M.M., Driscoll, T.B.: Neocytolysis: physiological down-regulator of red-cell mass. *Lancet* **349**(9062), 1389–90 (1997). [https://doi.org/10.1016/S0140-6736\(96\)09208-2](https://doi.org/10.1016/S0140-6736(96)09208-2)
- [35] Fu, Q., Shibata, S., Hastings, J.L., Platts, S.H., Hamilton, D.M., Bungo, M.W., Stenger, M.B., Ribeiro, C., Adams-Huet, B., Levine, B.D.: Impact of prolonged spaceflight on orthostatic tolerance during ambulation and blood pressure profiles in astronauts. *Circulation* **140**(9), 729–738 (2019). <https://doi.org/10.1161/CIRCULATIONAHA.119.041050>
- [36] Lukaski, H.C., Mendez, J., Buskirk, E.R., Cohn, S.H.: Relationship between endogenous 3-methylhistidine excretion and body composition. *Am J Physiol* **240**(3), 302–7 (1981). <https://doi.org/10.1152/ajpendo.1981.240.3.E302>
- [37] Young, V.R., Munro, H.N.: Ntau-methylhistidine (3-methylhistidine) and muscle protein turnover: an overview. *Fed Proc* **37**(9), 2291–300 (1978)
- [38] Kaur, I., Simons, E.R., Castro, V.A., Ott, C.M., Pierson, D.L.: Changes in monocyte functions of astronauts. *Brain Behav Immun* **19**(6), 547–54 (2005). <https://doi.org/10.1016/j.bbi.2004.12.006>
- [39] Crucian, B.E., Chouker, A., Simpson, R.J., Mehta, S., Marshall, G., Smith, S.M., Zwart, S.R., Heer, M., Ponomarev, S., Whitmire, A., Frippliat, J.P., Douglas, G.L., Lorenzi, H., Buchheim, J.I., Makedonas, G., Ginsburg, G.S., Ott, C.M., Pierson, D.L., Krieger, S.S., Baecker, N., Sams, C.: Immune system dysregulation during spaceflight: Potential countermeasures for deep space exploration missions. *Front Immunol* **9**, 1437 (2018). <https://doi.org/10.3389/fimmu.2018.01437>
- [40] Mehta, S.K., Szpara, M.L., Rooney, B.V., Diak, D.M., Shipley, M.M., Renner, D.W., Krieger, S.S., Nelman-Gonzalez, M.A., Zwart, S.R., Smith, S.M., Crucian, B.E.: Dermatitis during spaceflight associated with hsv-1 reactivation. *Viruses* **14**(4) (2022). <https://doi.org/10.3390/v14040789>
- [41] Mourad, M., Gershon, M., Mehta, S.K., Crucian, B.E., Hubbard, N., Zhang, J., Gershon, A.: Silent reactivation of varicella zoster virus in pregnancy: Implications for maintenance of immunity to varicella. *Viruses* **14**(7) (2022). <https://doi.org/10.3390/v14071438>

- [42] Mehta, S.K., Cohrs, R.J., Forghani, B., Zerbe, G., Gilden, D.H., Pierson, D.L.: Stress-induced subclinical reactivation of varicella zoster virus in astronauts. *J Med Virol* **72**(1), 174–9 (2004). <https://doi.org/10.1002/jmv.10555>
- [43] Mehta, S.K., Laudenslager, M.L., Stowe, R.P., Crucian, B.E., Sams, C.F., Pierson, D.L.: Multiple latent viruses reactivate in astronauts during space shuttle missions. *Brain Behav Immun* **41**, 210–7 (2014). <https://doi.org/10.1016/j.bbi.2014.05.014>
- [44] Wyss, M., Kaddurah-Daouk, R.: Creatine and creatinine metabolism. *Physiol Rev* **80**(3), 1107–213 (2000). <https://doi.org/10.1152/physrev.2000.80.3.1107>
- [45] Delanaye, P., Cavalier, E., Pottel, H.: Serum creatinine: Not so simple! *Nephron* **136**(4), 302–308 (2017). <https://doi.org/10.1159/000469669>
- [46] Green, R., Allen, L.H., Bjørke-Monsen, A.L., Brito, A., Gueant, J.L., Miller, J.W., Molloy, A.M., Nexo, E., Stabler, S., Toh, B.H., Ueland, P.M., Yajnik, C.: Vitamin b12 deficiency. *Nat Rev Dis Primers* **3**, 17040 (2017). <https://doi.org/10.1038/nrdp.2017.40>
- [47] Chu, C., Scanlon, P.: Vitamin b12 deficiency optic neuropathy detected by asymptomatic screening. *BMJ Case Rep* **2011** (2011). <https://doi.org/10.1136/bcr.02.2011.3823>
- [48] National Institutes of Health, O.o.D.S.: Phosphorus - Health Professional Fact Sheet (2022). <https://ods.od.nih.gov/factsheets/Phosphorus-HealthProfessional/#en33> Accessed 2022-04-09

Methods

Ethical approval.

All protocols described herein were reviewed and approved by the NASA Institutional Review Board (NASA eIRB study ID: STUDY00000201) and by Michigan State University (MSU) Biomedical and Health Institutional Review Board (MSU study ID: STUDY00003581) in accordance with the requirements of the Code of Federal Regulations on the Protection of Human Subjects. Written informed consent was obtained from all participating subjects (astronauts). All methods described in this investigation were carried out in accordance with the relevant guidelines and regulations. Additionally, approvals for data use and manuscript/data submission for the study were obtained from the Lifetime Surveillance of Astronaut Health (LSAH) advisory board.

Subjects

Forty-seven potential subjects were identified as U.S. astronauts that flew across 32 ISS and space shuttle expeditions and participated in two studies on Nutritional Status Assessment (SMO 016E), and Validation of Procedures for Monitoring Crewmember Immune Function (SMO 015). Thirty-eight astronauts agreed to participate following informed consent, and the analysis presented manuscript focuses on 27 subjects (20 male and 7 female) for whom long-duration measurements on the ISS were available (mean-based duration 165 days). Data for these subjects were obtained from LSAH and the Life Sciences Data Archive (LSDA).

Data preprocessing

To create non-attributable (deidentified) data, for each astronaut the different measurements were summarized into a maximum of 8 time points (using averages of measurements within each time bin). These measurement time bins were labeled as -180 and -45 days for pre-flight; early flight (33 days), mid-flight (82 days) and late flight (132 days) measurements; return (165 days), return+30 days (195 days) and return + 60 days (225 days). The binned data were then used for two comparisons: (I) individual astronaut analysis and (II) and across-astronaut comparison.

Individual astronaut analysis

Time series categorization.

The data from each individual astronaut were analyzed using PyI0mica's `calculateTimeSeriesCategorization` function ¹⁷. Here for each astronaut a , and each type of measurement m , the time series X_{ma} was analyzed, at time-points $t_i \in \{-180, -45, 33, 82, 132, 165, 195, 225\}$ days. For each X_{ma} the difference in intensity of each timepoint i was computed relative to the pre-flight

timepoint (-45 days) intensity, $\tilde{X}_{ma}(t_i) = X_{ma}(t_i) - X_{ma}(-45)$. Finally, X_{ma} was normalized using Euclidean norm to Q_{ma} , where $Q_{ma}(t_i) = \frac{\tilde{X}_{ma}(t_i)}{\sqrt{\sum_j (\tilde{X}_{ma}(t_j))^2}}$.

The `calculateTimeSeriesCategorization` algorithm uses spectral methods to classify time series^{12,17}: Internally, the Lomb-Scargle periodogram $P_{ma}(f)$ of each time series is computed at a series of frequencies f . The inverse Fourier transform of $P_{ma}(f)$ yields the autocorrelations, $\{\rho_{mal}\}$, at lags $l \in \{0, \dots, N/2\}$. A bootstrap time series set $B_{ja}(t)$, with $j \in \{1, \dots, 10^5\}$ is also generated (by sampling with replacement across the time series of each astronaut). By computing the autocorrelations of each $B_{ja}(t)$, null distributions at each lag l , and the corresponding 0.95 quantiles $\{\rho_{ql}\}$ are obtained. These quantiles are used to assign classes [*Lag M*], where M is the smallest lag for which the autocorrelation at lag l of a signal X_{ma} is greater than the corresponding bootstrap distribution quantile:

$$M = \text{Min} [\{l : \rho_{mal} \geq \rho_{ql}\}] . \quad (1)$$

The algorithm also checks whether time series X_{ma} that do not fulfill the criteria in Equation (1) have any pronounced intensity maxima or minima. Using again a bootstrap set of time series, the 0.95 quantiles \max_{qN} and \min_{qN} are computed, from the distributions of the maxima and minima of the bootstrap time series respectively. If $\max(X_{ma}) > \max_{qN}$, X_{ma} is assigned to class [*SpikeMax*]. If $\min(X_{ma}) < \min_{qN}$, X_{ma} is assigned to class [*SpikeMin*]. Time series assigned to any of the classes [*LagM*], [*SpikeMax*], and [*SpikeMin*] are considered to display statistically significant trends.

Cluster Categorization

For each time series class described above, PyI0mica's `clusterTimeSeriesCategorization` was used to further resolve the time trends, by implementing two levels of agglomerative hierarchical clustering: (i) First-level group (G) clustering uses autocorrelations ρ_{mal} as a vector for computing similarities (correlation based) (ii) Second-level Subgroup (S) clustering uses the normalized time series $\{Q_{ma}\}$ for computing similarities. The number of groups and subgroups within each class are determined by the silhouette method⁴⁹. For each astronaut and classification then results were summarized in heatmaps using `visualizeTimeSeriesCategorization` in PyI0mica. The [*Lag 1*] results from two astronauts are shown in Example outputs are shown in Figure 2. Full plots and corresponding measurements within each class are provided in the ODFs.

Cross-comparison of astronaut time series

Astronaut graph-based communities

Graph-based community analysis of the astronaut time series was performed¹⁸ with `networkx`⁵⁰ and `scikit-network`⁵¹. First, for each astronaut their time series periodograms P_{ma} were extracted using PyI0mica's `LombScargle` method. A distance matrix with components $[D_m]_{xy}$ was computed, for each measurement m and astronauts x, y , where the entries correspond to the Euclidean distance between P_{mx} and P_{my} . Again, a bootstrap set (50,000 signals) was constructed, and a distribution of distances between bootstrap time series was computed, with its 0.99th quantile d_q . Then the restricted distance matrix R_m entries were constructed, so that distances within a radius d_q were set to 1, and otherwise set to zero:

$$[R_m]_{xy} = \begin{cases} 1, & \text{if } [D_m]_{xy} < d_q \\ 0, & \text{if } [D_m]_{xy} \geq d_q \end{cases} \quad (2)$$

Using the restricted matrices for each measurement, a weighted adjacency matrix $A = \sum_m R_m$ was obtained. The adjacency matrix represents a graph with astronauts as vertices and edges that connect astronauts. Hence, in the graph, an edge E_{xy} joins two astronauts x, y if there is at least one time series measurement m for which the pairwise distance between the periodograms P_{mx} and P_{my} was smaller than d_q (i.e. there is similar temporal behavior). Finally, the edge E_{xy} is given a weight that corresponds to the number of measurements for which there is temporal similarity (i.e. the number of measurements m with non-zero entries in the restricted distance matrix corresponding entry $[R_m]_{xy}$, Equation (2)).

Graph community detection

The community structure of the astronaut graph constructed above was determined: First, a graph embedding with generalized singular value decomposition (GSVD, dimension 2) of the adjacency matrix was carried out in `scikit-network`. The `sklearn.metrics.silhouette_score` of⁵² was used to determine the number of components based on silhouette scores⁴⁹. Finally, a consensus network was constructed where the procedure was repeated 1000 times, and nodes were allocated to their highest frequency community membership (highest probability assignment).

Code and Data Availability

All data files and code used in this investigation, referred to as Online Data Files (ODFs) in the manuscript, have been deposited to and are available from the NASA Life Sciences Data Archive (LSDA). LSDA is the repository for all human and animal research data, including that associated with this study. LSDA has a public-facing portal where data requests can be initiated

(<https://nlsp.nasa.gov/explore/lsdahome/datarequest>). The LSDA team provides the appropriate processes, tools, and secure infrastructure for archival of experimental data and dissemination while complying with applicable rules, regulations, policies, and procedures governing the management and archival of sensitive data and information. The LSDA team enables data and information dissemination to the public or to authorized personnel either by providing public access to information or via an approved request process for information and data from the LSDA in accordance with NASA Human Research Program and Johnson Space Center (JSC) Institutional Review Board direction.

Additional Methods References

- [49] Rousseeuw, P.J.: Silhouettes: A graphical aid to the interpretation and validation of cluster analysis. *Journal of Computational and Applied Mathematics* **20**, 53–65 (1987). [https://doi.org/10.1016/0377-0427\(87\)90125-7](https://doi.org/10.1016/0377-0427(87)90125-7)
- [50] Hagberg, A.A., Schult, D.A., Swart, P.J.: Exploring network structure, dynamics, and function using networkx. In: Varoquaux, G., Vaught, T., Millman, J. (eds.) *Proceedings of the 7th Python in Science Conference*, Pasadena, CA USA, pp. 11–15 (2008). http://conference.scipy.org/proceedings/SciPy2008/paper_2/
- [51] Bonald, T., de Lara, N., Lutz, Q., Charpentier, B.: Scikit-network: Graph analysis in python, vol. 21, pp. 1–6 (2020). <http://jmlr.org/papers/v21/20-412.html>
- [52] Pedregosa, F., Varoquaux, G., Gramfort, A., Michel, V., Thirion, B., Grisel, O., Blondel, M., Prettenhofer, P., Weiss, R., Dubourg, V., Vanderplas, J., Passos, A., Cournapeau, D., Brucher, M., Perrot, M., Duchesnay, E.: Scikit-learn: Machine learning in Python, vol. 12, pp. 2825–2830 (2011). <http://jmlr.csail.mit.edu/papers/v12/pedregosa11a.html>